International Research Journal of Engineering and Technology (IRJET) e-ISSN: 2395-0056
Volume: 12 Issue: 04 | Apr 2025 www.irjet.net p-ISSN: 2395-0072

Morphological and linear viscoelastic properties of chitosan and multiwalled carbon nanotube nanocomposites.

J. R. González-Martínez[1], R. Gámez-Corrales[2], F. Barffuson-Dominguez[2], G.T. Paredes-Quijada[3]

[1]J.R. González-Martínez, Departamento de Investigación en Física, Universidad de Sonora, Apdo. Postal 1626, 83000 Hermosillo, Sonora, México.
[2]R. Gámez-Corrales, Professor, Departamento de Física, Universidad de Sonora, Apdo. Postal 1626, 83000, Hermosillo, Sonora, México. E-mail: rogelio.gamez@unison.mx.
[2]F. Barffuson-Dominguez, Departamento de Física, Universidad de Sonora, Apdo. Postal 1626, 83000, Hermosillo, Sonora, México.
[3]G.T Paredes-Quijada, Departamento de Ciencias Químico-Biológicas, Universidad de Sonora, Hermosillo, Sonora, México.

Abstract –

The present study investigates the morphological and linear rheological properties of chitosan and multi-walled carbon nanotubes (MWCNT) nanocomposites. A correlation is identified between the morphological properties of the nano aggregates induced by MWCNTs and their oscillatory linear rheology. The morphological properties were evaluated by atomic force microscopy. The linear rheological measurements were carried out as a function of the temperature range of 15 – 45ºC in aqueous solutions and are presented herein. Atomic force microscopy (AFM) was employed to ascertain the presence and extent of hierarchical self-assembled aggregated.

Key Words: Chitosan, MWCNT, nanoparticles, hierarchical structures, rheology, AFM.

1. INTRODUCTION

The utilization of natural polymers in industrial processes has increased significantly. This increase is driven by a need to develop environmentally friendly products. Chitosan, a polysaccharide composed of poly[β-(1-4)-2-amino-2-deoxy-D-glucopyranose] (see Figure 1), has emerged as a prominent agent in this field [1]. It is present in low concentrations in native chitin and is produced in varying degrees of deacetylation. Additionally, chitosan is present in certain fungal species [2], albeit in quantities lower than chitin. The deacetylation of chitin, a component of the exoskeleton of crustaceans such as shrimp, leads to the health engineering are notable, attributable to its antimicrobial, biocompatible, and biodegradable properties [3][4][5]. Studies have demonstrated that chitosan can promote wound healing [3]. In other fields of application, the removal of heavy metals from aqueous solutions has been demonstrated [6–8] . Conversely, the capacity of these natural materials to inhibit microbial growth suggests their potential use as biodegradable food packaging [9]. Given its innocuous nature, using chitin to combat fungi and bacteria has emerged as a viable strategy [10]. The data demonstrate the viability of the chains in terms of their size and the degree of their acetylation [11]. Given the inherent variability of these biopolymers, it is necessary to employ both molecular weight and average degree of deacetylation values for these biopolymers. The degree of deacetylation is a pivotal parameter in quantifying the relative concentration of amino groups within the polymer. A polymer containing less than 40% acetyl groups can be designated as chitosan or with a degree of deacetylation of 60%. Chitosan is a biocompatible, non-toxic, biodegradable polymer with film-forming and antimicrobial properties, rendering it a material with plenty of applications. One such application is extending the shelf life of fresh food products, including vegetables and meats, due to their high activity.

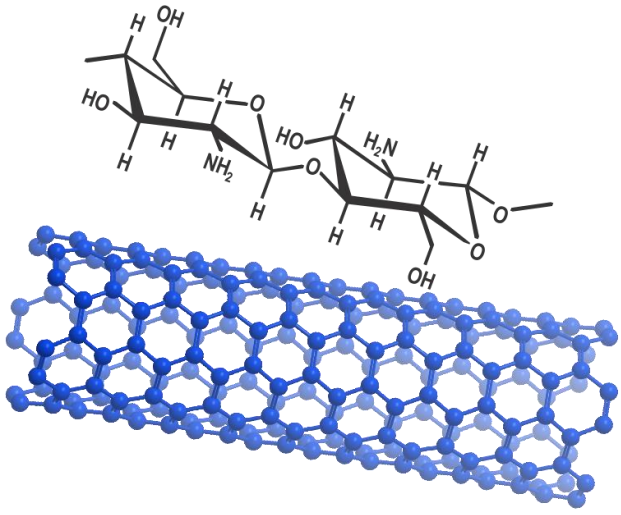

Figure 1 Schematic molecular structure of chitosan and carbon nanotube.

Carbon nanotubes are a class of nanomaterial composed of a sheet of benzene rings rolled on their axis[12] . These nanotubes can be rolled into one, two, or multiple layers, which impart distinct physicochemical properties,

regardless of the number of layers or the orientation of the benzene rings within the sheet of carbon atoms. These nanotubes are formed by curved, closed hexagonal carbon networks (Figure 1), consisting of nanometric carbon cylinders that exhibit fascinating properties that have attracted considerable interest from researchers in numerous technological applications [12]. These nanotubes exhibit a lightweight, hollow, and porous structure, along with high mechanical resistance, rendering them suitable for the structural reinforcement of materials. Their tensile strength and elasticity are noteworthy [13].

Most applications in which chitosan and CNTs are used require a material with excellent viscoelastic properties and control of its structure at the nanometric and micrometric scale [14][15][16]. The combination of these two materials results in nanocomposites with improved properties. The mechanical properties of the nanocomposites, such as Young's modulus, tensile strength, and elongation, are significantly improved by adding MWCNTs[17] . Pure chitosan multilayer films exhibited substantially lower tensile strength and elongation than pure chitosan solid films. However, the relative improvement in mechanical properties of the porous MWCNT/chitosan multilayer nanocomposites was higher, especially in elongation, which showed a twofold improvement in deformation [18]. The strain rate sensitivity of the films was also investigated, and it was observed that the viscoelastic behavior of the multilayered and foamed pure chitosan could become more pronounced with increasing strain rate [19]. On the other hand, the interaction between the chitosan polymer chains and the surface-modified MWCNTs could dampen the viscoelastic properties. In addition to the mechanical properties [16], it was found that these materials are not cytotoxic to osteoblasts, suggesting that they may hold promise for tissue engineering applications [20]. The potential of MWCNT-reinforced chitosan nanocomposites as multifunctional materials with enhanced properties. Their ability to improve mechanical, thermal, and biological properties makes them promising candidates for various applications, including tissue engineering [21], drug delivery[22], and biomedical devices[23].

This study comprehensively examines the linear oscillatory rheology of chitosan and the material's morphology in the presence of multi-walled carbon nanotubes (MWCNTs). Atomic force microscopy facilitates the characterization of morphology.

2. EXPERIMENTAL DETAILS

2.1 Sample preparations

The study used three molecular weights of chitosan (low, medium, and high, 70-190 kDa, 190-310 kDa, and 310-390 kDa, respectively) and MWCNT. The chitosan and MWCNT powders were obtained from Sigma-Aldrich and employed without prior purification. The solvent mixture comprised a solution of ultrapure water (with an electrical conductivity of at least 18.2 MΩ/cm) and acetic acid (pH of 4.5).

2.2 Atomic Force Microscopy

A drop was placed on a metal grid and allowed to dry before being observed in an atomic force microscope (AFM) JEOL JSPM-4210. All the AFM measurements were performed in a tapping mode with a frequency of 325 kHz, and a constant force of 40 N with a tip of 8 nm.

2.3 Rheological measurements

The linear rheological properties were determined in a controlled strain mode utilizing an Anton Paar MCR 300 rheometer with a cone-plate geometry (cone angle 0.98° and 50.0 mm of diameter). The Temperature was maintained using control conducted using a Peltier system (TEK150P-C), and a humidification chamber was employed to prevent alterations in sample composition resulting from solvent evaporation during the measurements. All measurements were conducted within a frequency range of 0.1 and 100 rad/s.

3. RESULTS AND DISCUSSION

3.1 Atomic Force Microscopy

Figure 2 shows the morphology of low molecular weight chitosan as observed through atomic force microscopy (AFM) at room temperature. The dissolution process employs a solvent mixture comprising acetic acid and water (66%) to facilitate the dissolution of low molecular weight chitosan.

Figure 2B shows filiform hierarchical aggregates of a smaller size than those observed in the high and medium-molecular-weight chitosan solution systems. The aggregates have a diameter of 2.0mm, which is approximately one order of magnitude smaller than that observed in previous samples (no images included). Furthermore, the length exceeds 3.0 mm. In contrast, the radius of chitosan nanoparticles is 50nm, as illustrated in the background of Figure 2C. It should be noted that the position of the carbon nanotubes is not discernible in this image. Furthermore, it is feasible to differentiate between the aggregates. The aggregates were observed to form zones or regions larger than 4.0 mm, comprising aggregates smaller than the abovementioned, with a diameter of approximately 0.6 mm for the medium and high molecular weight. These observations indicate that the aggregates coexist as components of a physical gel, which will be presented in greater detail in the subsequent subsection on linear oscillatory rheology. In light of the observations mentioned earlier, we postulate that the

interaction between these aggregates is the underlying cause of the observed increase in system viscosity (see the rheological measurements subsection).

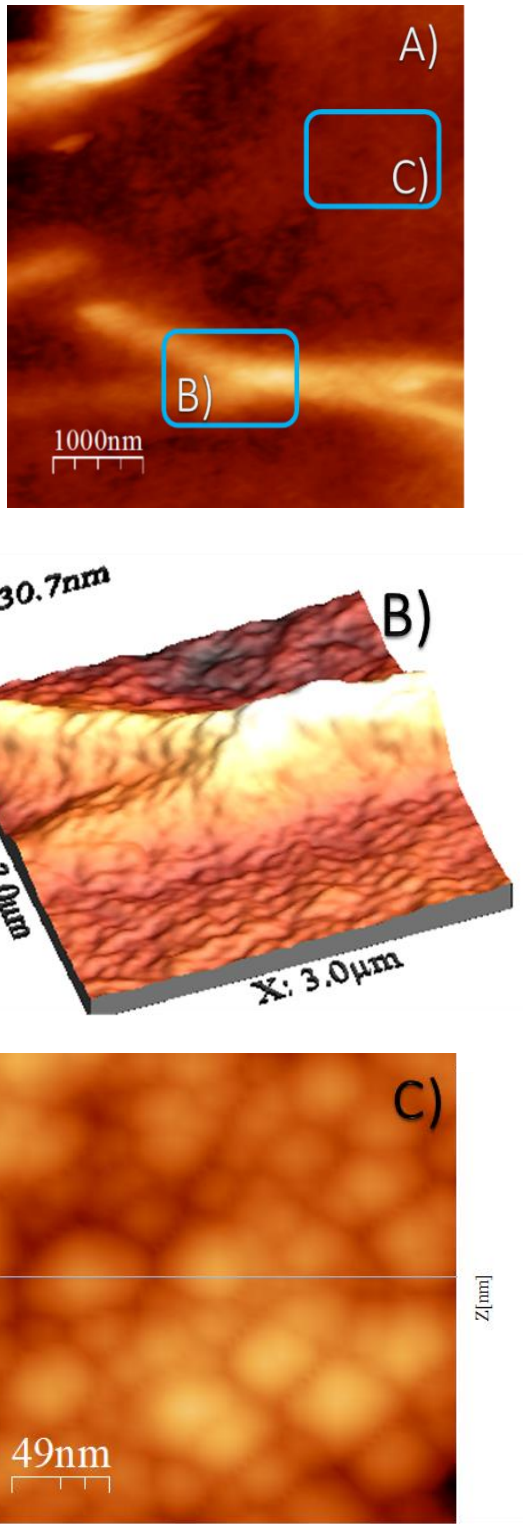

Figure 2 shows an AFM image of MWCNT and chitosan of low molecular weight at room temperature.

3.2 Rheological measurements

All viscoelasticity measurements were conducted in the linear stress versus strain regime using a rheometer that applies a strain at a constant, controlled temperature, under standard practice. This is the regime in which Hooke's law is an appliance. The temperature was applied from 15 to 40°C. It was observed that the viscoelastic behavior of the systems composed of medium molecular weight chitosan dissolved in a mixture of acetic acid and water exhibited distinct characteristics compared to those observed in high molecular weight chitosan solutions. All rheological measurements were conducted with the percentage of MWCNT held constant. It should be noted that all temperature measurements were performed at identical values, precisely 15, 20, 25, 30, 35, and 40 degrees Celsius. The linear viscoelastic behaviors observed in this system are considerably complex as shown in Figure 3. In this system, a viscoelastic behavior is observed that can be governed by two distinct regimes, each with the same number of underlying physical origins. At low frequencies (below 1 rad/s, approximately), the rheological behavior is characterized by an elastic modulus greater than the viscous modulus. In contrast, there is an increasing behavior above the values of 1 rad/s, where the viscous modulus is greater than the elastic one. The two moduli exhibit a nearly parallel slope, with the value of the slope slightly higher than that of the viscous modulus. The two zones are associated with the transition regime, while the zone corresponding to high frequencies is associated with the breathing regime. However, work was avoided above that temperature, and even measurements at 40°C were conducted rapidly to control the evaporation of the solvent. This allowed for the concentration and viscoelastic properties of the system to remain consistent.

Figure 4 shows the viscoelastic behavior of chitosan and MWCNT samples with a high molecular weight at a temperature of 15°C. As can be observed, all linear oscillatory rheological measurements were conducted within a frequency range of 0.1 to 100 rad/s. In all measurements, a viscous modulus greater than the elastic modulus was observed, indicating that the system exhibited viscoelastic behavior rather than viscous elastic behavior. At frequencies exceeding 100 rad/s, the two moduli would intersect, which can be attributed to the fact that the relaxation times are less than 0.01 seconds. In contrast, the gradients of G' and G'' are analogous to those of the Maxwell model, though not precisely equal to 2 and 1, respectively . Upon thermalization of the system to a temperature of 40°C, a tendency for the module values to be almost parallel with a slope less than 1 is observed.

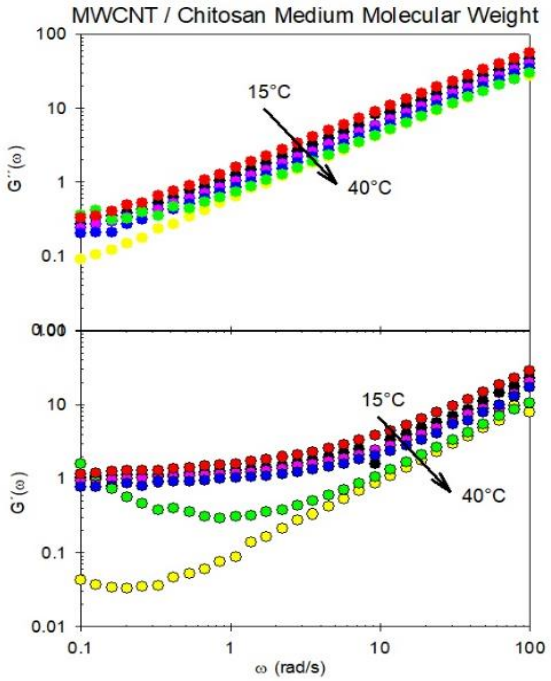

Figure 3 Loss (G´´) and storage (G´) characteristics of chitosan of medium molecular weight as a function of the angular frequency and controlled temperature (15°C-40°C).

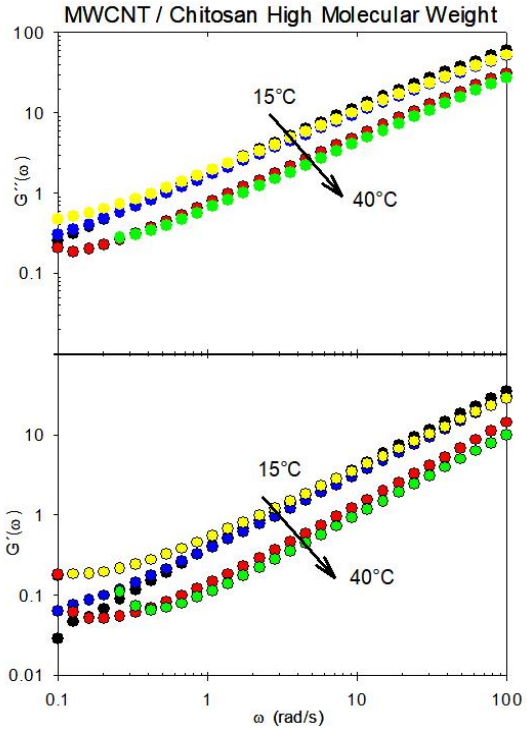

Figure 4 shows the loss (G´´) and storage (G´) characteristics of high-molecular-weight chitosan as a function of the angular frequency and controlled temperature (15°C-40°C).

The viscoelastic behaviors of the systems composed of medium molecular weight chitosan dissolved in a mixture of acetic acid and water exhibit distinctive characteristics compared to those observed in high molecular weight chitosan solutions. The linear viscoelastic behaviors observed in this novel system are considerably more complex than those illustrated in Figure 3. In this novel system, a viscoelastic behavior is observed that can be governed by two distinct regimes, each with the same number of underlying physical origins. At low frequencies (below 1 rad/s, approximately), the rheological behavior is distinguished by an elastic modulus greater than the viscous modulus. In contrast, there is an increasing behavior above the value of 1 rad/s, whereby the viscous modulus is greater than the elastic one. The two moduli exhibit a nearly parallel slope slightly with an elastic modulus higher than the viscous modulus. The two zones are associated with the transition regime, while the high frequencies zone corresponds to the breathing regime.

Figures 3 and 4 demonstrate that the data points representing the module values at various temperatures exhibit a near-perfect collapse on a master curve. This suggests that the viscoelastic behavior observed in the system has a single underlying physical cause, manifesting in the distinct viscoelastic regimes previously described.

4 CONCLUSIONS

In conclusion, this study examined the morphology of chitosan nano aggregates induced by MWCNT nanotubes and their correlation with their linear oscillatory rheological properties. Atomic force microscopy (AFM) images demonstrated that the system comprising chitosan and multi-walled carbon nanotubes (MWCNTs) resulted in spherical chitosan nanoparticles, which the MWCNTs induced. The aggregate diameter was determined to be 50 nm. Furthermore, the formation of hierarchical structures comprising spherical aggregates was observed to reach lengths of several microns. The main results of the linear oscillatory rheological measurements indicated that the system exhibited the characteristics of a transient physical gel, with a temperature dependence. An Arrhenius-like dependence is observed, which involves an activation energy in the different MWCNT-chitosan complexes. This dependence is indicative of associativity, whereby the formation of aggregates is primarily attributed to the associative interaction of the chitosan-carbon nanotube self-assembly composites.

REFERENCES

1. E. P. Milan, V. C. A. Martins, M. M. Horn, & A. M. G. Plepis, Influence of blend ratio and mangosteen extract in chitosan/collagen gels and scaffolds: Rheological and release studies. *Carbohydrate Polymers*, **292** (2022). https://doi.org/10.1016/j.carbpol.2022.119647.

2. R. Rodríguez-Rodríguez, H. Espinosa-Andrews, C. Velasquillo-Martínez, & Z. Y. García-Carvajal, Composite hydrogels based on gelatin, chitosan and polyvinyl alcohol to biomedical applications: a review. *International Journal of Polymeric Materials and Polymeric Biomaterials*, **69** (2020) 1–20. https://doi.org/10.1080/00914037.2019.1581780.

3. R. A. A. Muzzarelli, P. Morganti, G. Morganti, P. Palombo, M. Palombo, G. Biagini, M. Mattioli Belmonte, F. Giantomassi, F. Orlandi, & C. Muzzarelli, Chitin nanofibrils/chitosan glycolate composites as wound medicaments. *Carbohydrate Polymers*, **70** (2007) 274–284. https://doi.org/10.1016/j.carbpol.2007.04.008.

4. 2019 Biomaterials Chitosan cancer. (n.d.).

5. J. Venkatesan & S. K. Kim, Chitosan composites for bone tissue engineering - An overview. *Marine Drugs*, **8** (2010) 2252–2266. https://doi.org/10.3390/md8082252.

6. M. A. Salam, M. S. I. Makki, & M. Y. A. Abdelaal, Preparation and characterization of multi-walled carbon nanotubes/chitosan nanocomposite and its application for the removal of heavy metals from aqueous solution. *Journal of Alloys and Compounds*, **509** (2011) 2582–2587. https://doi.org/10.1016/j.jallcom.2010.11.094.

7. T. Zhao, X. Ji, W. Jin, S. Guo, Y. Cheng, X. Wang, A. Dang, H. Li, & T. Li, Electrochemical performance of chitosan oligosaccharide/carbon nanotube composite for detection of trace copper(II) ion. *International Journal of Electrochemical Science*, **12** (2017) 1808–1817. https://doi.org/10.20964/2017.03.35.

8. A. B. López-Oyama, M. A. Domínguez-Crespo, A. M. Torres-Huerta, E. Onofre-Bustamante, R. Gámez-Corrales, N. Cayetano-Castro, & A. C. Ferrel-Álvarez, Dataset on electrochemical reduced graphene oxide production: Effect of synthesis parameters. *Data in Brief*, **21** (2018) 598–603. https://doi.org/10.1016/j.dib.2018.10.014.

9. J. Mikešová, J. Hašek, G. Tishchenko, & P. Morganti, Rheological study of chitosan acetate solutions containing chitin nanofibrils. *Carbohydrate Polymers*, **112** (2014) 753–757. https://doi.org/10.1016/j.carbpol.2014.06.043.

10. M. E. I. Badawy, E. I. Rabea, A. R. Eid, M. M. Badr, & G. I. K. Marei, Structure and antimicrobial comparison between N-(benzyl) chitosan derivatives and N-(benzyl) chitosan tripolyphosphate nanoparticles against bacteria, fungi, and yeast. *International Journal of Biological Macromolecules*, **186** (2021) 724–734. https://doi.org/10.1016/J.IJBIOMAC.2021.07.086.

11. C. Iamsamai, S. Hannongbua, U. Ruktanonchai, A. Soottitantawat, & S. T. Dubas, The effect of the degree of deacetylation of chitosan on its dispersion of carbon nanotubes. *Carbon*, **48** (2010) 25–30. https://doi.org/10.1016/j.carbon.2009.06.060.

12. 1991 Nature Ijima CNT. (n.d.).

13. M. J. O'connell, P. Boul, L. M. Ericson, C. Hu□man, Y. Wang, E. Haroz, C. Kuper, J. Tour, K. D. Ausman, & R. E. Smalley, *Reversible water-solubilization of single-walled carbon nanotubes by polymer wrapping*.

14. Y. Otsubo, M. Fujiwara, M. Kouno, & K. Edamura, Shear-thickening flow of suspensions of carbon nanofibers in aqueous PVA solutions. *Rheologica Acta*, **46** (2007) 905–912. https://doi.org/10.1007/s00397-007-0173-z.

15. M. K. Tiwari, A. V. Bazilevsky, A. L. Yarin, & C. M. Megaridis, Elongational and shear rheology of carbon nanotube suspensions. *Rheologica Acta*, **48** (2009) 597–609. https://doi.org/10.1007/s00397-009-0354-z.

16. Y. Liu, J. Tang, X. Chen, & J. H. Xin, Decoration of carbon nanotubes with chitosan. *Carbon*, **43** (2005) 3178–3180. https://doi.org/10.1016/j.carbon.2005.06.020.

17. E. K. Hobbie, Shear rheology of carbon nanotube suspensions. *Rheologica Acta*, **49** (2010) 323–334. https://doi.org/10.1007/s00397-009-0422-4.

18. M. K. Tiwari, A. V. Bazilevsky, A. L. Yarin, & C. M. Megaridis, Elongational and shear rheology of carbon nanotube suspensions. *Rheologica Acta*, **48** (2009) 597–609. https://doi.org/10.1007/s00397-009-0354-z.

19. C. Tang, L. Xiang, J. Su, K. Wang, C. Yang, Q. Zhang, & Q. Fu, Largely improved tensile properties of chitosan film via unique synergistic reinforcing effect of carbon nanotube and clay. *Journal of Physical Chemistry B*, **112** (2008) 3876–3881. https://doi.org/10.1021/jp709977m.

20. M. L. Pita-López, G. Fletes-Vargas, H. Espinosa-Andrews, & R. Rodríguez-Rodríguez, Physically cross-linked chitosan-based hydrogels for tissue engineering applications: A state-of-the-art review.

European Polymer Journal, **145** (2021). https://doi.org/10.1016/j.eurpolymj.2020.110176

21. M. M. Islam, M. Shahruzzaman, S. Biswas, M. Nurus Sakib, & T. U. Rashid, Chitosan based bioactive materials in tissue engineering applications-A review. *Bioactive Materials*, **5** (2020) 164–183. https://doi.org/10.1016/j.bioactmat.2020.01.012.

22. I. Singha & A. Basu, Chitosan based injectable hydrogels for smart drug delivery applications. *Sensors International*, **3** (2022). https://doi.org/10.1016/j.sintl.2022.100168.

23. N. Desai, D. Rana, S. Salave, R. Gupta, P. Patel, B. Karunakaran, A. Sharma, J. Giri, D. Benival, & N. Kommineni, Chitosan: A Potential Biopolymer in Drug Delivery and Biomedical Applications. *Pharmaceutics*, **15** (2023). https://doi.org/10.3390/pharmaceutics15041313
.